BMC Cancer

RESEARCH

Open Access

# SKA1/2/3 is a prognostic and predictive biomarker in esophageal adenocarcinoma and squamous cell carcinoma

Liming Zhang[1,2], Shaoqiang Wang[3] and Lina Wang[1,4*]

## Abstract

**Background** Esophageal carcinoma (ESCA) ranks among the most prevalent malignant tumors globally. Despite significant advancements in treatment options and improved patient outcomes, the 5-year survival rate remains unsatisfactory. The spindle and kinetochore associated complex subunit 1/2/3 (SKA1/2/3) attached to the kinetochore (KT) in the metaphase of mitosis are implicated in the occurrence and development of various tumors. However, the expression patterns, diagnostic significance and prognostic implications of SKA1/2/3 in ESCA have not been comprehensively determined.

**Methods** TCGA, UALCAN, Kaplan-Meier Plotter, and TIMER databases were leveraged to dissect the expression patterns, prognostic implications and diagnostic value of SKA1/2/3 in ESCA patients, as well as to investigate the potential regulatory mechanism of SKA1/2/3 in the onset and progression of ESCA.

**Results** In ESCA, SKA1/2/3 exhibited substantial expression, with higher levels relating significantly with clinicopathological features and patient prognosis. Enrichment analysis of genes co-expressed with SKA1/2/3 highlighted their involvement in the cell cycle, DNA replication and p53 signaling pathway. Protein-protein interaction (PPI) analysis identified ten hub genes that were not only markedly upregulated but also portended a poor prognosis in ESCA. Additionally, immune infiltration assays uncovered a significant link between SKA1/2/3 expression and the immune cell infiltration within ESCA. Silencing of SKA1/2/3 significantly suppresses cell proliferation and migration, while concurrently promoting apoptosis in ESCA cells.

**Conclusions** SKA1/2/3 may serve as promising biomarkers for the prognosis and diagnosis of ESCA, which holds promise as a novel therapeutic target for the disease.

**Keywords** SKA1/2/3, Esophageal carcinoma (ESCA), Prognostic biomarker, Diagnosis, Bioinformatics analysis

*Correspondence:
Lina Wang
wanglina_china@163.com
[1]Medical Research Center, Affiliated Hospital of Jining Medical University, Jining Medical University, Jining, Shandong Province 272029, P. R. China
[2]Department of Thoracic Surgery, Weifang Second People's Hospital, Weifang, Shandong Province 261041, P. R. China
[3]Department of Thoracic Surgery, Weifang People's Hospital, Weifang, Shandong Province 261000, P. R. China
[4]Medical Research Center, Affiliated Hospital of Jining Medical University, 89 Guhuai Road, Jining, Shandong Province 272029, China

## Introduction

Esophageal carcinoma (ESCA) is among the most commonly diagnosed malignant tumors of the digestive system globally. The latest statistics indicate that its incidence rate is seventh, while the mortality rate stands sixth worldwide. ESCA is categorized into two main pathological subtypes: esophageal adenocarcinoma (EAC) and esophageal squamous cell carcinoma (ESCC) [1]. Despite the availability of various treatment options for ESCA, the 5-year survival rate for patients remains below 20%, primarily due to drug resistance and metastatic spread [2, 3]. Consequently, there is an urgent need to identify early diagnostic biomarkers, explore novel therapeutic targets, and enhance our understanding of the etiology and progression of ESCA.

SKA1, SKA2, and SKA3 constitute the spindle and kinetochore-associated complex subunit (SKA) family, which plays a crucial role in maintaining the attachment between intermediate spindle microtubules and centromeres, thereby ensuring the proper completion of mitosis [4, 5]. Recent research has identified the SKA family as a novel group of cancer-related proteins implicated in the progression of various malignancies. Specifically, SKA1 has been shown to foster the growth and invasion of bladder cancer by inhibiting CDK4 and Cyclin D1, thereby blocking the activation of ERK2 and AKT pathways [6]. In papillary thyroid carcinoma (PTC), high expression levels of SKA1 have been correlated with poor patient prognosis [7]. In hepatocellular carcinoma (HCC), SKA2 is highly expressed and can stimulate tumor growth and invasion by triggering the b-catenin signaling pathway [8]. Furthermore, SKA3 enhances the AKT signaling pathway to boost glycolysis and counteract the development of laryngeal squamous cell carcinoma (LSCC), especially in the context of chemotherapy resistance. This is achieved by binding to Polo-like kinase 1 (PLK1), thereby preventing ubiquitin-mediated degradation [9]. Thus, SKA1/2/3 may serve as a prognostic biomarker. However, to date, limited research has explored the potential significance of SKA1/2/3 in the etiology, progression, and prognosis of ESCA.

In this study, we conducted an analysis of SKA1/2/3 expression in ESCA and investigated its relation with clinicopathological characteristics. Subsequently, we identified co-expressed genes and explored the potential underlying biological mechanisms. The aim of our research is to generate insights that may contribute to the discovery of new biomarkers for the diagnosis and prognosis of ESCA, as well as to identify potential therapeutic targets for this disease.

## Materials and methods

### Expression of SKA1/2/3 in ESCA and its relation with clinicopathological features

The UALCAN database (http://ualcan.path.uab.edu/index.html) is a thorough, interactive and user-friendly web tool for studying cancer OMICS data [10]. Log into the website, choose "TCGA", enter "SKA1/2/3", choose "Esophageal carcinoma" from the list of TCGA datasets, and click "Links for analysis" under "Expression" to learn more about the expression of SKA1/2/3 in ESCA, as well as the relationship between SKA1/2/3 expression and clinicopathological features including cancer stage, tumor grade and nodal metastasis.

### The prognostic significance of SKA1/2/3 in ESCA

The Kaplan-Meier plotter (http://www.kmplot.com) combines chip data from GEO, TCGA and other databases to offer predictive data for a variety of cancers [11]. To examine the relationship between the expression of SKA1/2/3 and the prognosis of ESCA, we performed a database search on the K-M plotter platform.

### The diagnostic value of SKA1/2/3 in ESCA

To explore the potential diagnostic value of SKA1/2/3 in ESCA, the R pROC package was utilized. We downloaded the RNAseq data of the ESCA project in the HTSeq-FPKM format from TCGA database, converted to TPM with log2 transformation, then used the ggplot2 package to analyze and visualize the results to build the receiver operating characteristic (ROC) curves.

### GO and KEGG enrichment analysis of SKA1/2/3 co-expressed genes in ESCA

We obtained the data of the ESCA project in TCGA, filtered the sample data, eliminated the samples from the control group and the normal group, then performed an analysis by the stat package for the R language. The ggplot2 was used to depict the 10 genes with the strongest connections. To identify genes with strong association with SKA1/2/3, the Pearson correlation coefficients ($|r| > 0.4$ and $P<0.001$) were used as screening thresholds. The overlapping of the SKA1/2/3 genes was found in the Wayne diagram. To investigate the potential biological activities and signal transduction pathways of SKA1/2/3, we utilized the R language cluster Profiler package for gene ontology (GO) and Kyoto encyclopedia of genes and genomes (KEGG) enrichment analysis of SKA1/2/3-related genes and the org.Hs.eg.db package for ID conversion. Visit the BioPlot website (https://www.chiplot.online/) to obtain the results.

### Construction of PPI network with SKA1/2/3 co-expressed genes in ESCA

The STRING database (https://cn.string-db.org) is used to anticipate and search the known protein-protein interactions (PPI) [12]. The PPI network of genes associated with SKA1/2/3 was created by STRING (v11.5) and Cytoscape (v3.9.1) [13].

### Immune infiltration analysis of SKA1/2/3 in ESCA

Download the RNA-seq data and clinical information of the ESCA project from TCGA database. Subsequently, process the data, excluding normal samples. Extract the expression data of SKA1/2/3, and utilize MCP-counter and the ssGSEA algorithm from the GSVA package to analyze immune cell infiltration.

The TIMER database (https://cistrome.shinyapps.io/timer/) contains 10,897 tissue samples and 32 tumors from TCGA database [14]. It can comprehensively examine both the genes connected to the tumor and the relationship between malignancies and immune cell infiltration. We used the TIMER website to search the connection between SKA1/2/3 expression and immune infiltration in ESCA as well as the distribution of immune subsets in ESCA for each copy number.

### Clinical sample collection

Tumor and adjacent non-tumorous tissues of 40 patients with ESCA, who underwent surgical treatment in the Department of Thoracic Surgery, Affiliated Hospital of Jining Medical University from Oct 2020 to Sept 2022, were collected. This study was approved by the Ethics Committee of the Affiliated Hospital of Jining Medical University (Approval number 2021-11-C009) in accordance with the Declaration of Helsinki. All 40 ESCA patients signed written informed consent and did not receive other special treatment before surgery.

### Quantitative reverse transcription-polymerase chain reaction (qRT- PCR)

Total tissue RNA of patients was collected according to the instructions of Trizol kit (Invitrogen), and cDNA was synthesized with the reverse transcription kit (Vazyme). The expression of SKA1, SKA2 and SKA3 was detected by qRT-PCR. GAPDH was used as internal control. Primer sequences are as follows.

| **SKA1 forward:** | **5′-CCTGAACCCGTAAAGAAGCCT-3′** |
|---|---|
| SKA1 reverse: | 5′-TCATGTACGAAGGAACACCATTG-3′ |
| SKA2 forward: | 5′- GCCGCATTTGTGCTACTGTG-3′ |
| SKA2 reverse: | 5′- CTCTGCCGCAGTTTTCTCTT-3′ |
| SKA3 forward: | 5′- TGAGCGGTACATCGTATCCCA-3′ |
| SKA3 reverse: | 5′- GGGGTTACAATTACGGGCTCT-3′ |
| GAPDH forward: | 5′-GGAGCGAGATCCCTCCAAAAT-3′ |
| GAPDH reverse: | 5′-GGCTGTTGTCATACTTCTCATGG-3′ |

### Tissue microarray (TMA)

The ESCA tissues and paracancerous tissues were embedded in paraffin. Continuous 4 mm slices were dewaxing, plugging, incubating with the primary antibody overnight at 4°C; then adding the secondary antibody, incubating at room temperature for 2 h, then analyzing the signals. The human ESCA tissue microarray was provided by Shanghai Zhuoli Biotechnology Co., Ltd. (Shanghai, China), and SKA1/2/3 expression was assessed by an automated VisioMorph system (Visiopamm ®, Hoersholm, Denmark).

### Cell culture and transfection

| | **Si-1** | **SKA1–Homo-896** | **S: 5′-GGGAGGACU UACUCGUUAUTT-3′** |
|---|---|---|---|
| SKA1 | | | AS: 5′-AUAACGAGUA AGUCCUCCCTT-3′ |
| | Si-2 | SKA1–Homo-621 | S: 5′-CGCUUAACCUA UAAUCAAATT-3′ |
| | | | AS: 5′-UUUGAUUA UAGGUUAAGCGTT-3′ |
| | Si-1 | SKA2-Homo-65 | S: 5′-CUGAGUCUGA UCUGGAUUATT-3′ |
| SKA2 | | | AS: 5′-UAAUCCAGAU CAGACUCAGTT-3′ |
| | Si-2 | SKA2-Homo-355 | S: 5′-GAGCAAUUCAA AUUUCACATT-3′ |
| | | | AS: 5′-UGUGAAAUU UGAAUUGCUCTT-3′ |
| | Si-1 | SKA3-Homo-602 | S: 5′-CAGGCAGUGA ACAACUAUATT-3′ |
| SKA3 | | | AS: 5′-UAUAGUUG UUCACUGCCUGTT-3′ |
| | Si-2 | SKA3-Homo-840 | S: 5′-CCAGGCUCAAU GAUAAUGUTT-3′ |
| | | | AS: 5′-ACAUUAUCAU UGAGCCUGGTT-3′ |

Human ESCA cell line KYSE-150 and KYSE-450 were cultured in a 37°C $CO_2$ incubator using RPMI 1640 medium supplemented with 10% fetal bovine serum. KYSE-150 and KYSE-450 cells were plated in a six-well plate, and siRNA was mixed with Lipofectamine 3000 before adding into the medium for transfection. The siRNA sequences for SKA1, SKA2, and SKA3 are as follows.

### Cell proliferation assay by cell counting kit-8 (CCK-8)

$2\times10^3$ cells were seeded into a 96-well plate after 48 h siRNA transfection, and incubated in a standard cell culture incubator. A 10 μL CCK-8 solution was added to each well at 0 h, 24 h, 48 h, and 72 h, followed by incubation at 37°C for 2 h. The absorbance at 450 nm was analyzed with standard microplate readers (BioTek, Winsky, Vermont, USA).

### Scratch wound healing assay

Six-well plates with a cell density of $5\times10^5$ cells per well after siRNA transfection were used. After covering the monolayer, the cells were scratched with the 10 μL tips of the pipette and washed in PBS. The culture medium without FBS was added to continue the culture. The pictures were taken under a microscope at 0 h and 24 h, and analyzed by ImageJ software.

### Detection of apoptosis by flow cytometry

$3\times10^5$ cells were inoculated in a six-well plate for siRNA transfection. The Annexin $V^+$ cells underwent apoptosis were detected by flow cytometry after 48 h post-transfection.

### Statistical analysis

SPSS 20.0 software was used for statistical analysis with GraphPad Prism 9 software for graphing. Normally distributed measurement data are expressed as mean±standard deviation (SD), *t*-test was performed for the intergroup comparison. Rank sum test was used to compare the measurement data groups that did not conform to normal distribution. $P<0.05$ was statistically significant.

## Results

### Expression of SKA1/2/3 in ESCA and its relation with clinicopathological features

The mRNA expression of SKA1/2/3 in ESCA was firstly investigated by scanning UALCAN database. The findings demonstrated that ESCA had considerably high levels of SKA1/2/3 expression ($P<0.001$) (Fig. 1A-C). Notably, SKA1 and SKA2 exhibited significantly elevated expression levels in ESCC compared to EAC. However, there was no significant difference observed in the expression of SKA3 (Fig. 1D-F). This indicates that SKA1/2/3 might be connected to the emergence and progression of ESCA. The patient characteristics of ESCA provides a clear and concise overview of the demographic and clinical features of all the ESCA patients (Table 1 and Supplementary Table 1). The relationship between SKA1/2/3 expression and clinicopathological characteristics, such as tumor stage and lymph node metastasis, was further explored. A substantial relation between the expression of SKA1/2/3 with clinicopathological stages was discovered. Tumor stage 4 had the highest levels of SKA1/3 expression, while stage 2 with the highest levels of SKA2 (Fig. 1G-I). Similarly, there was a relation between the expression of SKA1/2/3 and the lymph node metastasis. The highest level of SKA1/3 expression was seen in N3, and the highest SKA2 in N2 (Fig. 1J-L). Thus, the elevated expression of SKA1/2/3 was significantly associated with clinicopathological features in ESCA.

### The prognostic values of SKA1/2/3 in ESCA

The Kaplan-Meier website was searched to explore the prognostic values of SKA1/2/3 in ESCA. Firstly, we analyzed the relationship between SKA1/2/3 expression and EAC overall survival (OS) and recurrence-free survival (RFS). The high expression of SKA1 (HR=2.34, Logrank $P=0.05$) and SKA3 (HR=3.21, Logrank $P=0.0015$) was closely related to adverse OS in EAC patients, while SKA2 (HR=2.01, Logrank $P=0.09$) was not significantly correlated (Fig. 2A-C). There was no significant correlation between the expression of SKA1 (HR=0.4, Logrank $P=0.42$), SKA2 (HR=2.47, Logrank $P=0.42$), or SKA3 (HR=3.37, Logrank $P=0.21$) with RFS in EAC patients (Fig. 2D-F). In ESCC patients, the high expression of SKA1 (HR=0.16, Logrank $P=0.0011$) and SKA3 (HR=0.37, Logrank $P=0.017$) were related to favorable OS, with no significant relation between SKA2 (HR=0.53, Logrank $P=0.13$) and ESCC OS (Fig. 2G-I). The elevated expression of SKA3 (HR=2.66, Logrank $P=0.037$) was linked to poor RFS with no significant relation between SKA1 (HR=0.44, Logrank $P=0.081$), and SKA2 (HR=2.42, Logrank $P=0.072$) (Fig. 2J-L) in ESCC. Upon combining ESCC and EAC, we observed no significant differences between the high and low expression groups of SKA1/2/3, with the exception of the progression free interval for SKA3 (Supplementary Fig. 1A-I). Thus, elevated expression of SKA1/3 is associated with poor OS in EAC, yet it surprisingly correlates with favorable OS in ESCC. Conversely, high levels of SKA3 expression are linked to an unfavorable RFS in ESCC.

### The diagnostic significance of SKA1/2/3 in ESCA

ROC curves were created to assess the diagnostic utility of SKA1/2/3 in ESCA patients. The area under the curve (AUC) is 0.939 (95%CI: 0.861-1.000), 0.936 (95%CI: 0.864-1.000), and 0.961 (95%CI: 0.918-1.000), respectively (Fig. 3A-C). We also explored the diagnostic values of SKA1/2/3 in EAC and ESCC. In EAC patients, the AUC is 0.917 (95%CI: 0.804-1.000), 0.902 (95%CI: 0.780-1.000), and 0.960 (95%CI: 0.911-1.000), respectively (Fig. 3D-F). In ESCC patients, the AUC is 0.963, 0.988, and 0.976, respectively (Fig. 3G-I). Since AUC has low accuracy at 0.5 to 0.7, moderate accuracy at 0.7 to 0.9, and high accuracy above 0.9, SKA1/2/3 has considerable predictive ability for ESCA, no matter whether it's EAC or ESCC.

### Construction of PPI network with SKA1/2/3 co-expressed genes with exploration of the expression and prognosis of the hub genes

We screened out 710 SKA1 co-expressed genes, 410 SKA2 co-expressed genes, and 712 SKA3 co-expressed genes with data from TCGA (Supplementary Table 2). The intersection of 204 SKA1/2/3 co-expressed genes

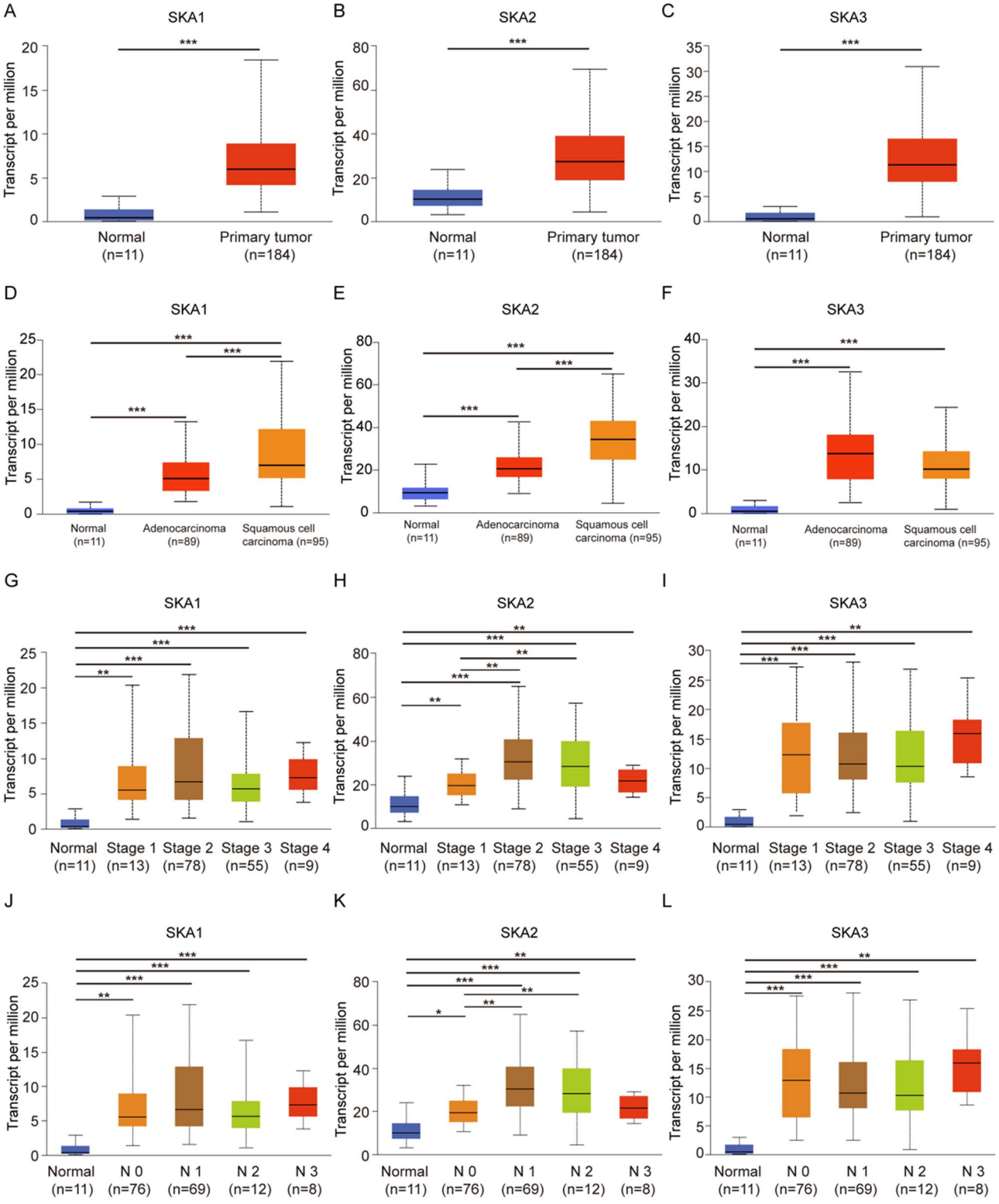


**Fig. 1** Expression of SKA1/2/3 in ESCA and the relation with clinicopathological features in UALCAN (A-C) Expression of SKA1/2/3 in ESCA. (D-F) SKA1/2/3 expression based on ESCA histology. (G-I) SKA1/2/3 expression in relation to individual cancer stages. (J-L) SKA1/2/3 expression related to lymph node metastasis. *$P < 0.05$, **$P < 0.01$; ***$P < 0.001$

**Table 1** The patient characteristics of ESCA from TCGA

| characteristics | Low expression of SKA1 | High expression of SKA1 | *P* value | Low expression of SKA2 | High expression of SKA2 | *P* value | Low expression of SKA3 | High expression of SKA3 | *P* value |
|---|---|---|---|---|---|---|---|---|---|
| n | 81 | 82 | | 81 | 82 | | 81 | 82 | |
| Pathologic T stage, n (%) | | | 0.30218027 | | | 0.145904183 | | | 0.759825313 |
| T1 | 17 (11.7%) | 10 (6.9%) | | 18 (12.4%) | 9 (6.2%) | | 14 (9.7%) | 13 (9%) | |
| T2 | 16 (11%) | 21 (14.5%) | | 15 (10.3%) | 22 (15.2%) | | 21 (14.5%) | 16 (11%) | |
| T3 | 41 (28.3%) | 36 (24.8%) | | 37 (25.5%) | 40 (27.6%) | | 39 (26.9%) | 38 (26.2%) | |
| T4 | 1 (0.7%) | 3 (2.1%) | | 1 (0.7%) | 3 (2.1%) | | 3 (2.1%) | 1 (0.7%) | |
| Pathologic N stage, n (%) | | | 0.30542589 | | | 0.379451074 | | | 0.200087982 |
| N0 | 32 (22.2%) | 34 (23.6%) | | 28 (19.4%) | 38 (26.4%) | | 38 (26.4%) | 28 (19.4%) | |
| N1 | 30 (20.8%) | 33 (22.9%) | | 33 (22.9%) | 30 (20.8%) | | 28 (19.4%) | 35 (24.3%) | |
| N2 | 7 (4.9%) | 2 (1.4%) | | 6 (4.2%) | 3 (2.1%) | | 7 (4.9%) | 2 (1.4%) | |
| N3 | 4 (2.8%) | 2 (1.4%) | | 2 (1.4%) | 4 (2.8%) | | 3 (2.1%) | 3 (2.1%) | |
| Pathologic M stage, n (%) | | | 1 | | | 0.600070168 | | | 0.209302745 |
| M0 | 63 (48.8%) | 58 (45%) | | 56 (43.4%) | 65 (50.4%) | | 66 (51.2%) | 55 (42.6%) | |
| M1 | 4 (3.1%) | 4 (3.1%) | | 5 (3.9%) | 3 (2.3%) | | 2 (1.6%) | 6 (4.7%) | |
| Pathologic stage, n (%) | | | 0.77838481 | | | 0.387647197 | | | 0.401116822 |
| Stage I | 9 (6.3%) | 7 (4.9%) | | 10 (7%) | 6 (4.2%) | | 9 (6.3%) | 7 (4.9%) | |
| Stage II | 32 (22.5%) | 37 (26.1%) | | 29 (20.4%) | 40 (28.2%) | | 36 (25.4%) | 33 (23.2%) | |
| Stage III | 27 (19%) | 22 (15.5%) | | 24 (16.9%) | 25 (17.6%) | | 28 (19.7%) | 21 (14.8%) | |
| Stage IV | 4 (2.8%) | 4 (2.8%) | | 5 (3.5%) | 3 (2.1%) | | 2 (1.4%) | 6 (4.2%) | |
| Clinical T stage, n (%) | | | 0.26680624 | | | 0.637457035 | | | 0.255383118 |
| T1 | 3 (5.8%) | 3 (5.8%) | | 3 (5.8%) | 3 (5.8%) | | 4 (7.7%) | 2 (3.8%) | |
| T2 | 5 (9.6%) | 5 (9.6%) | | 3 (5.8%) | 7 (13.5%) | | 6 (11.5%) | 4 (7.7%) | |
| T3 | 10 (19.2%) | 22 (42.3%) | | 9 (17.3%) | 23 (44.2%) | | 11 (21.2%) | 21 (40.4%) | |
| T4 | 0 (0%) | 4 (7.7%) | | 2 (3.8%) | 2 (3.8%) | | 1 (1.9%) | 3 (5.8%) | |
| Clinical N stage, n (%) | | | 0.55516941 | | | 0.478591684 | | | 0.305212741 |
| N0 | 8 (18.6%) | 9 (20.9%) | | 3 (7%) | 14 (32.6%) | | 8 (18.6%) | 9 (20.9%) | |
| N1 | 7 (16.3%) | 16 (37.2%) | | 8 (18.6%) | 15 (34.9%) | | 10 (23.3%) | 13 (30.2%) | |
| N2 | 1 (2.3%) | 2 (4.7%) | | 1 (2.3%) | 2 (4.7%) | | 0 (0%) | 3 (7%) | |
| Clinical M stage, n (%) | | | 0.94451004 | | | 0.004715357 | | | 1 |
| M0 | 14 (26.9%) | 27 (51.9%) | | 9 (17.3%) | 32 (61.5%) | | 16 (30.8%) | 25 (48.1%) | |
| M1 | 3 (5.8%) | 8 (15.4%) | | 8 (15.4%) | 3 (5.8%) | | 4 (7.7%) | 7 (13.5%) | |
| Clinical stage, n (%) | | | 0.50924214 | | | 0.006131696 | | | 0.666235514 |
| Stage I | 2 (3.7%) | 1 (1.9%) | | 2 (3.7%) | 1 (1.9%) | | 2 (3.7%) | 1 (1.9%) | |
| Stage II | 8 (14.8%) | 13 (24.1%) | | 4 (7.4%) | 17 (31.5%) | | 9 (16.7%) | 12 (22.2%) | |
| Stage III | 5 (9.3%) | 14 (25.9%) | | 4 (7.4%) | 15 (27.8%) | | 6 (11.1%) | 13 (24.1%) | |
| Stage IV | 3 (5.6%) | 8 (14.8%) | | 8 (14.8%) | 3 (5.6%) | | 4 (7.4%) | 7 (13%) | |
| Primary therapy outcome, n (%) | | | 0.02177042 | | | 0.073296045 | | | 0.170988927 |
| PD | 2 (2.1%) | 8 (8.5%) | | 7 (7.4%) | 3 (3.2%) | | 4 (4.3%) | 6 (6.4%) | |

**Table 1** (continued)

| characteristics | Low expression of SKA1 | High expression of SKA1 | *P* value | Low expression of SKA2 | High expression of SKA2 | *P* value | Low expression of SKA3 | High expression of SKA3 | *P* value |
|---|---|---|---|---|---|---|---|---|---|
| n | 81 | 82 | | 81 | 82 | | 81 | 82 | |
| SD | 6 (6.4%) | 1 (1.1%) | | 4 (4.3%) | 3 (3.2%) | | 5 (5.3%) | 2 (2.1%) | |
| PR | 0 (0%) | 3 (3.2%) | | 0 (0%) | 3 (3.2%) | | 0 (0%) | 3 (3.2%) | |
| CR | 32 (34%) | 42 (44.7%) | | 27 (28.7%) | 47 (50%) | | 40 (42.6%) | 34 (36.2%) | |
| Gender, n (%) | | | 0.79737682 | | | 0.108116441 | | | 0.797376824 |
| Female | 12 (7.4%) | 11 (6.7%) | | 15 (9.2%) | 8 (4.9%) | | 12 (7.4%) | 11 (6.7%) | |
| Male | 69 (42.3%) | 71 (43.6%) | | 66 (40.5%) | 74 (45.4%) | | 69 (42.3%) | 71 (43.6%) | |
| Race, n (%) | | | 0.20741052 | | | 2.71454E-05 | | | 0.670550701 |
| Asian | 15 (10.3%) | 23 (15.9%) | | 6 (4.1%) | 32 (22.1%) | | 20 (13.8%) | 18 (12.4%) | |
| Black or African American | 2 (1.4%) | 4 (2.8%) | | 4 (2.8%) | 2 (1.4%) | | 2 (1.4%) | 4 (2.8%) | |
| White | 55 (37.9%) | 46 (31.7%) | | 59 (40.7%) | 42 (29%) | | 52 (35.9%) | 49 (33.8%) | |
| Age, n (%) | | | 0.00012442 | | | 0.001324902 | | | 0.050338314 |
| <= 60 | 29 (17.8%) | 54 (33.1%) | | 31 (19%) | 52 (31.9%) | | 35 (21.5%) | 48 (29.4%) | |
| > 60 | 52 (31.9%) | 28 (17.2%) | | 50 (30.7%) | 30 (18.4%) | | 46 (28.2%) | 34 (20.9%) | |
| BMI, n (%) | | | 0.03667935 | | | 5.5423E-05 | | | 0.42688791 |
| <= 25 | 35 (22.7%) | 49 (31.8%) | | 29 (18.8%) | 55 (35.7%) | | 45 (29.2%) | 39 (25.3%) | |
| > 25 | 41 (26.6%) | 29 (18.8%) | | 47 (30.5%) | 23 (14.9%) | | 33 (21.4%) | 37 (24%) | |
| Histological type, n (%) | | | 0.00612461 | | | 8.0461E-07 | | | 0.182836061 |
| Adenocarcinoma | 49 (30.1%) | 32 (19.6%) | | 56 (34.4%) | 25 (15.3%) | | 36 (22.1%) | 45 (27.6%) | |
| Squamous Cell Carcinoma | 32 (19.6%) | 50 (30.7%) | | 25 (15.3%) | 57 (35%) | | 45 (27.6%) | 37 (22.7%) | |
| Residual tumor, n (%) | | | 0.26946346 | | | 0.238908523 | | | 0.510337728 |
| R0 | 66 (49.3%) | 55 (41%) | | 59 (44%) | 62 (46.3%) | | 66 (49.3%) | 55 (41%) | |
| R1 | 5 (3.7%) | 6 (4.5%) | | 7 (5.2%) | 4 (3%) | | 4 (3%) | 7 (5.2%) | |
| R2 | 0 (0%) | 2 (1.5%) | | 0 (0%) | 2 (1.5%) | | 1 (0.7%) | 1 (0.7%) | |
| Histologic grade, n (%) | | | 0.4022523 | | | 0.007338215 | | | 0.24686158 |
| G1 | 5 (3.9%) | 11 (8.7%) | | 3 (2.4%) | 13 (10.2%) | | 11 (8.7%) | 5 (3.9%) | |
| G2 | 33 (26%) | 33 (26%) | | 25 (19.7%) | 41 (32.3%) | | 33 (26%) | 33 (26%) | |
| G3 | 21 (16.5%) | 24 (18.9%) | | 27 (21.3%) | 18 (14.2%) | | 20 (15.7%) | 25 (19.7%) | |
| Smoker, n (%) | | | 0.95341414 | | | 0.442962799 | | | 0.595592903 |
| No | 24 (16.6%) | 24 (16.6%) | | 21 (14.5%) | 27 (18.6%) | | 26 (17.9%) | 22 (15.2%) | |
| Yes | 48 (33.1%) | 49 (33.8%) | | 49 (33.8%) | 48 (33.1%) | | 48 (33.1%) | 49 (33.8%) | |
| Alcohol history, n (%) | | | 0.53346395 | | | 0.602571165 | | | 0.782884413 |
| No | 25 (15.6%) | 22 (13.8%) | | 25 (15.6%) | 22 (13.8%) | | 24 (15%) | 23 (14.4%) | |
| Yes | 54 (33.8%) | 59 (36.9%) | | 55 (34.4%) | 58 (36.2%) | | 55 (34.4%) | 58 (36.2%) | |
| Reflux history, n (%) | | | 0.61435249 | | | 0.090308163 | | | 0.523854992 |
| No | 42 (30.7%) | 43 (31.4%) | | 38 (27.7%) | 47 (34.3%) | | 44 (32.1%) | 41 (29.9%) | |
| Yes | 28 (20.4%) | 24 (17.5%) | | 31 (22.6%) | 21 (15.3%) | | 24 (17.5%) | 28 (20.4%) | |
| Tumor cental location, n (%) | | | 0.06542721 | | | 0.002164993 | | | 0.435143159 |

**Table 1** (continued)

| characteristics | Low expression of SKA1 | High expression of SKA1 | *P* value | Low expression of SKA2 | High expression of SKA2 | *P* value | Low expression of SKA3 | High expression of SKA3 | *P* value |
|---|---|---|---|---|---|---|---|---|---|
| n | 81 | 82 | | 81 | 82 | | 81 | 82 | |
| Distal | 63 (38.9%) | 51 (31.5%) | | 66 (40.7%) | 48 (29.6%) | | 55 (34%) | 59 (36.4%) | |
| Mid | 17 (10.5%) | 25 (15.4%) | | 15 (9.3%) | 27 (16.7%) | | 24 (14.8%) | 18 (11.1%) | |
| Proximal | 1 (0.6%) | 5 (3.1%) | | 0 (0%) | 6 (3.7%) | | 2 (1.2%) | 4 (2.5%) | |

was visualized by a Wayne diagram (Fig. 4A). PPI network of the SKA1/2/3 co-expressed genes was built in Cytoscape by STRING, with ten hub genes obtained: CDK1, CCNB1, CDC45, NDC80, CCNA2, AURKB, DLGAP5, RAD51, RFC4, and BUB1B (Fig. 4B). Subsequent search on UALCAN revealed that the expression of all hub genes was noticeably elevated in ESCA ($P<0.001$) (Supplementary Fig. 2A-J). To investigate the relationship between these hub gene expression and ESCA prognosis, we found a substantial correlation between high expression of CDK1, CCNB1, NDC80, AURKB, DLGAP5, RAD51, RFC4, and BUB1B with the unfavorable prognosis of EAC patients, while a significant correlation between elevated expression of CDK1, CCNB1, CDC45, NDC80, CCNA2, DLGAP5, RAD51, and BUB1B with the favorable prognosis of ESCC patients (Supplementary Fig. 3).

### GO and KEGG enrichment analysis of SKA1/2/3 co-expressed genes in ESCA

In order to further understand the potential roles of SKA1/2/3 in ESCA, we carried out GO and KEGG enrichment analysis of SKA1/2/3 co-expressed genes. The main biological process of these genes was focused on nuclear division, organelle fission, chromosome segregation, and DNA replication. They primarily have function in catalytic activity, DNA helicase activity, and ATPase activity, with cellular location in the chromosomal region, centromeric region, and kinetochore (Fig. 4C-E). KEGG enrichment analysis showed that SKA1/2/3 expression is linked to several important pathways, such as cell cycle, DNA replication, and p53 signaling pathway (Fig. 4F).

### Immuno-infiltration analysis SKA1/2/3 in ESCA

MCP-counter was used to explore the immune cell infiltration of SKA1/2/3 in ESCA. Based on SKA1/2/3 mRNA expression, TCGA samples were split into high and low expression groups by median. The MCP-counter revealed significant difference in $CD8^+$ T cell, T cell, and myeloid dendritic cell infiltration between SKA1 high and low expression groups (Fig. 5A). Additionally, difference in neutrophil and T cell infiltration was observed in SKA2 high and low expression groups (Fig. 5B). Furthermore, distinctions in monocyte, NK cell, T cell, myeloid dendritic cell, and endothelial cell infiltration was found between SKA3 high and low expression groups (Fig. 5C). Subsequently, we employed the ssGSEA algorithm and Spearman analysis to investigate the correlation between SKA1/2/3 expression and the infiltration of 24 distinct immune cell types. SKA1 showed strong positive relation to Th2 and Tgd cells, while negative to mast cells, eosinophils, pDC, $CD8^+$ T cells, neutrophils, Th17 cells, iDC, cytotoxic cells, T cells, DC, Tem, TFH, B cells, NK

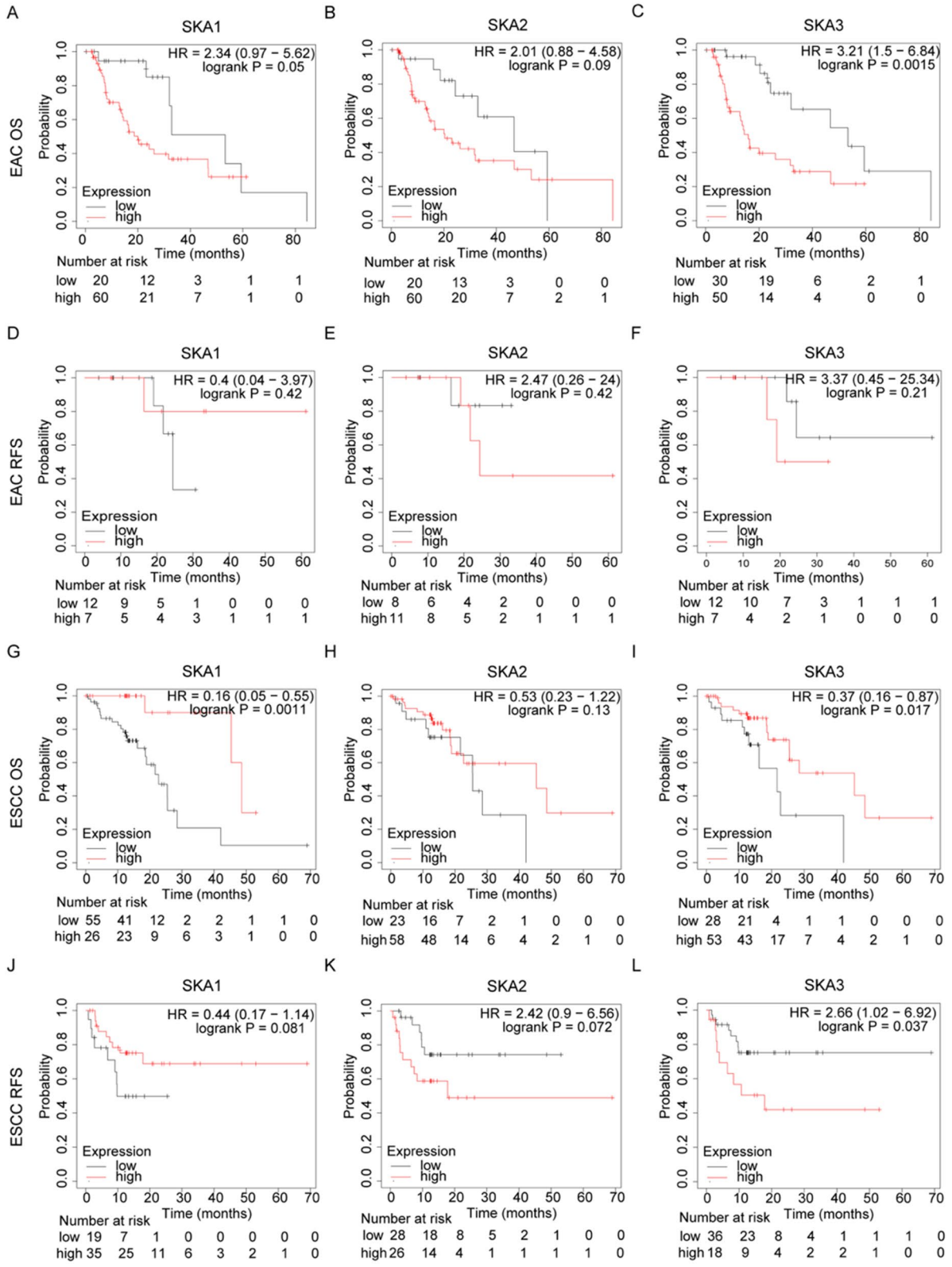


**Fig. 2** The prognostic values of SKA1/2/3 in ESCA from Kaplan-Meier plotter. (**A-C**) The relationship between SKA1/2/3 expression and EAC OS. (**D-F**) The relationship between SKA1/2/3 expression and EAC RFS. (**G-I**) The relationship between SKA1/2/3 expression and ESCC OS. (**J-L**) The relationship between SKA1/2/3 expression and ESCC RFS

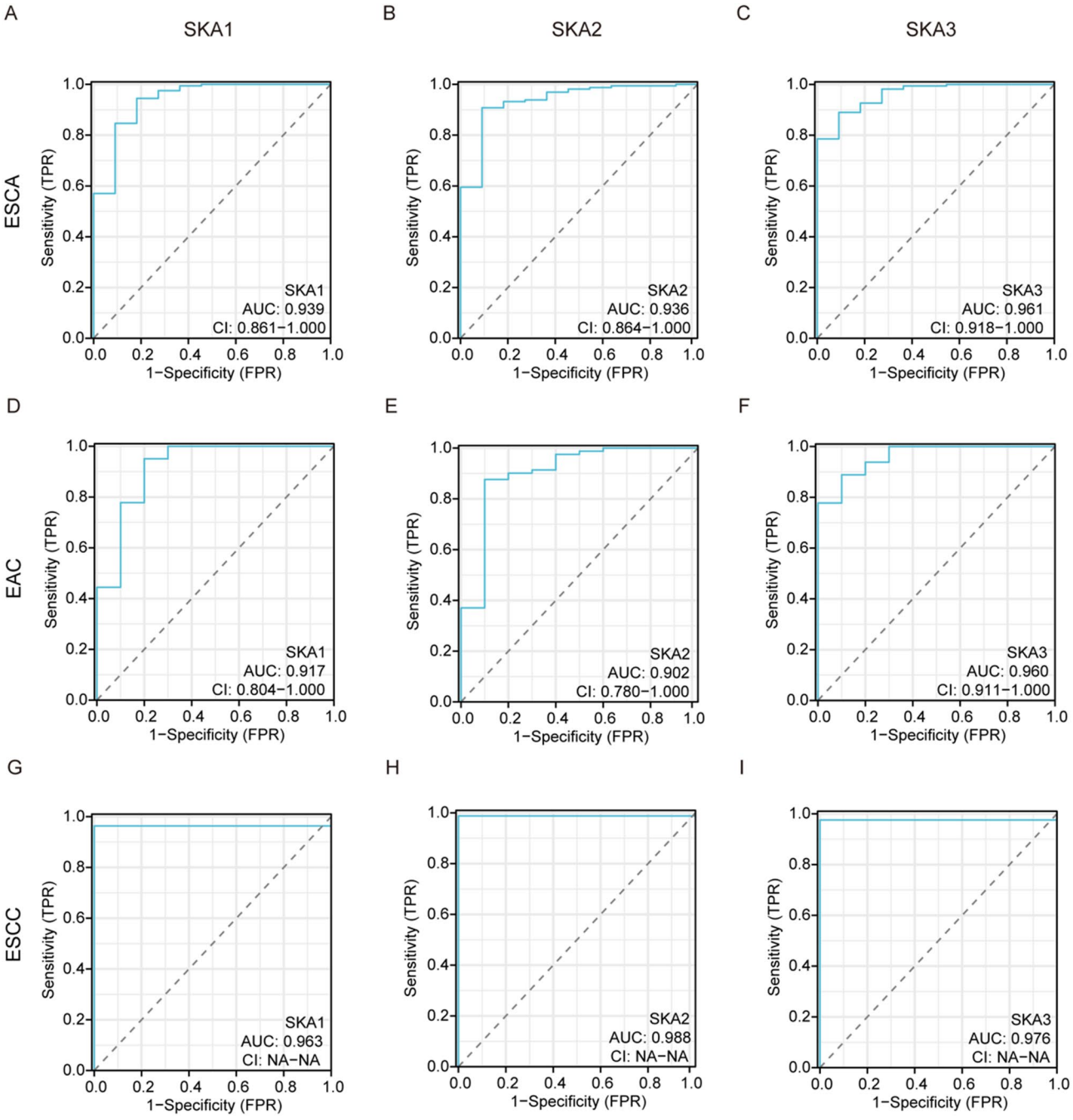


**Fig. 3** The diagnostic value of SKA1/2/3 in ESCA patients. The ROC curve of SKA1/2/3 in ESCA (**A-C**), EAC (**D-F**), and ESCC (**G-I**)

CD56bright cells, and macrophages. SKA2 revealed positive correlation to Th2, Tcm, Tgd, and NK cells, with negative to Th17 cells, eosinophils, NK CD56bright cells, neutrophils, pDC, mast cells, B cells, $CD8^+$ T cells, Tem, TFH, and T cells. SKA3 demonstrated positive association with Th2 cells, while negative with mast cells, cytotoxic cells, iDC, $CD8^+$ T cells, DC, pDC, TFH, NK CD56dim cells, neutrophils, T cells, macrophages, Tcm, Th1 cells, aDC, Treg, NK cells, B cells, and eosinophils (Fig. 5D-F, and Supplementary Fig. 4).

In addition, the TIMER database showed that the expression of SKA1 was negatively correlated with $CD8^+$ T cells, neutrophils, and dendritic cells but not with B cells, $CD4^+$ T cells, or macrophages. SKA2 expression was positively correlated with macrophages but not with B cells, $CD8^+$ T cells, $CD4^+$ T cells, neutrophils, or dendritic cells. The expression of SKA3 was positively correlated with B cells while negatively with neutrophils and dendritic cells, but not with $CD8^+$ T cells, $CD4^+$ T cells, or macrophages (Supplementary Fig. 5A). Moreover,

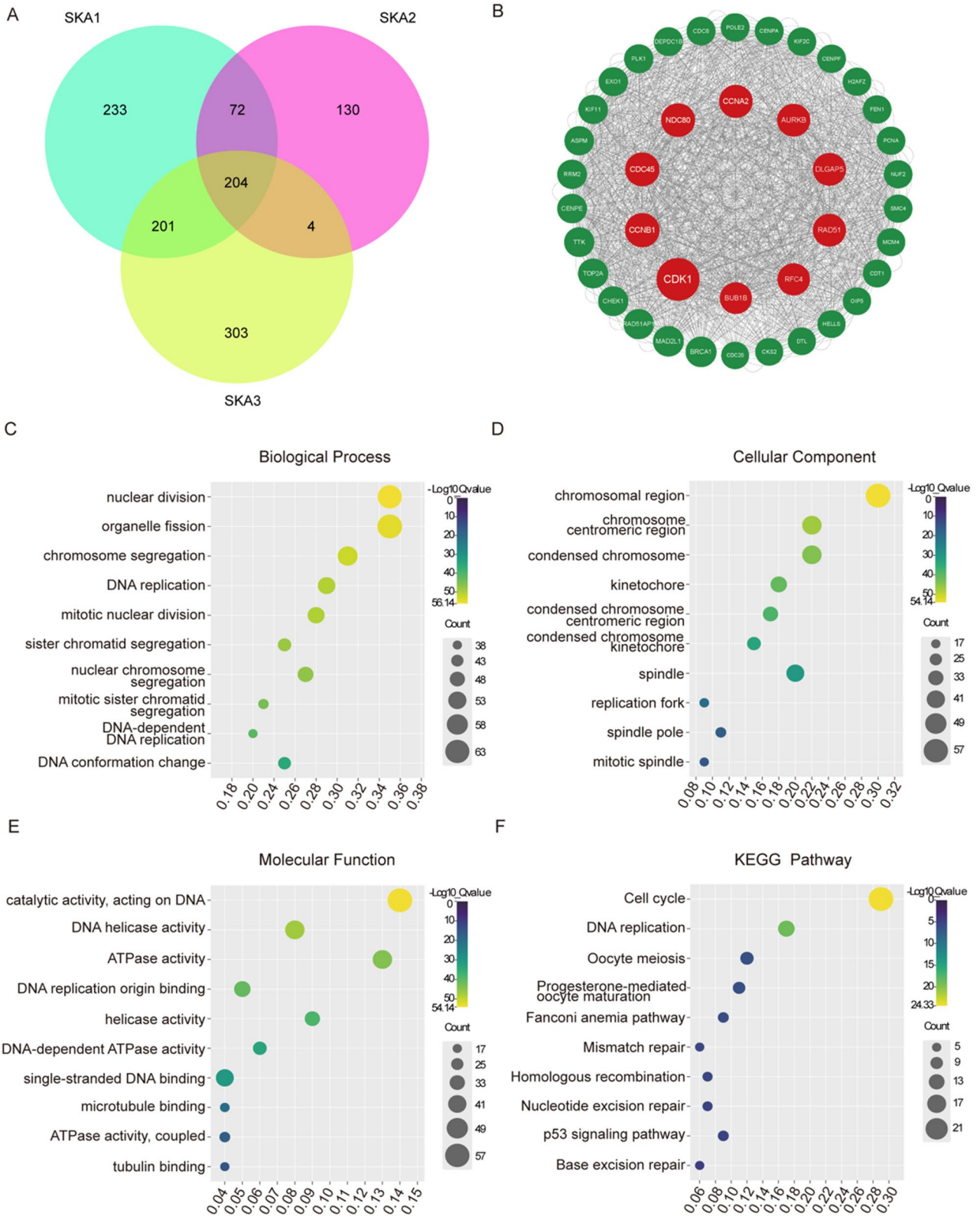


**Fig. 4** GO and KEGG enrichment analysis of SKA1/2/3 co-expressed genes(**A**) Intersection of co-expressed genes of SKA1/2/3 in ESCA. (**B**) PPI network of SKA1/2/3 co-expressed genes. Biological process (**C**), Cellular component (**D**), Molecular function (**E**), and KEGG pathway (**F**) of SKA1/2/3 co-expressed genes

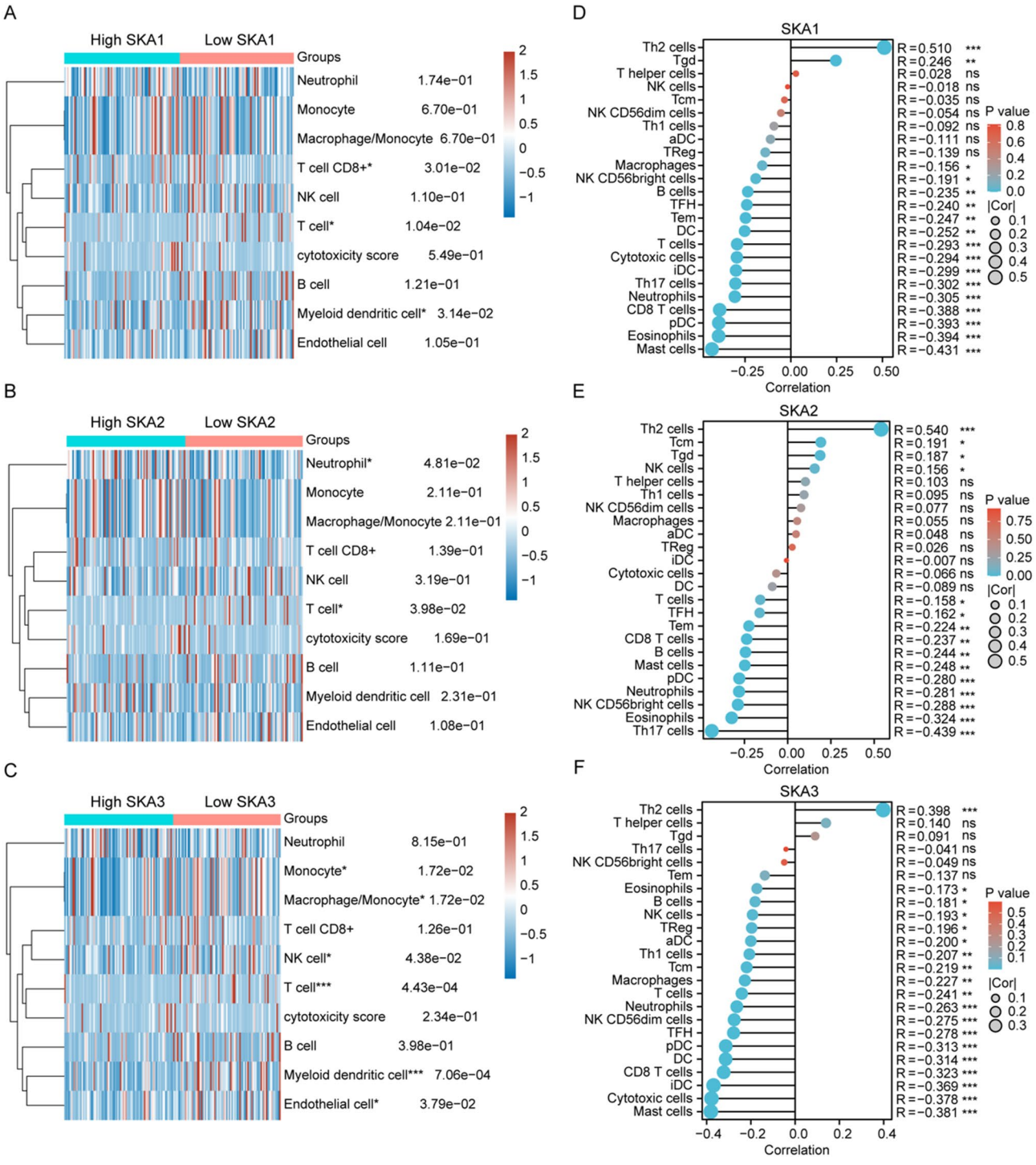


**Fig. 5** Immuno-infiltration analysis SKA1/2/3 in ESCA (**A-C**) Correlation between SKA1/2/3 expression and the infiltration of immune cells by MCP-counter, and ssGSEA (**D-F**)

different copy states of SKA1/2/3 have certain effects on immune infiltration (Supplementary Fig. 5B-D).

### Verification of SKA1/2/3 mRNA and protein expression in ESCA specimens

To validate the mRNA and protein expression of SKA1/2/3 in ESCA, qRT-PCR and tissue microarray analysis (TMA) was performed. The 40 paired ESCA and non-cancerous tissues were used to detect SKA1/2/3

mRNA levels by qRT-PCR, and the correlation between their expressions with clinical pathological features was analyzed (Supplementary Table 3). SKA1 was substantially elevated in 24 of the 40 ESCA tissues ($P=0.001$). The mRNA levels of SKA2 and SKA3 were increased in 25 and 27 ESCA tissues with statistical significance (SKA2: $P=0.023$; SKA3: $P=0.041$) (Fig. 6A-C). SKA2 mRNA expression was significantly correlated with the age ($P=0.040$), and that of SKA2/3 was significantly associated with the tumor size in ESCA patients (SKA2: $P<0.001$; SKA3: $P=0.004$) (Supplementary Table 3).

In addition, the TMA showed that SKA1/2/3 protein levels were significantly elevated in ESCA tissues compared to non-cancerous tissues by H-score (Fig. 6D-I). Additionally, we have further substantiated our findings by conducting an analysis of GSE75241 dataset, comprising samples from ESCA and adjacent non-cancerous tissues. It revealed that the mRNA expression levels of SKA1/2/3 were notably higher in ESCA tissues compared

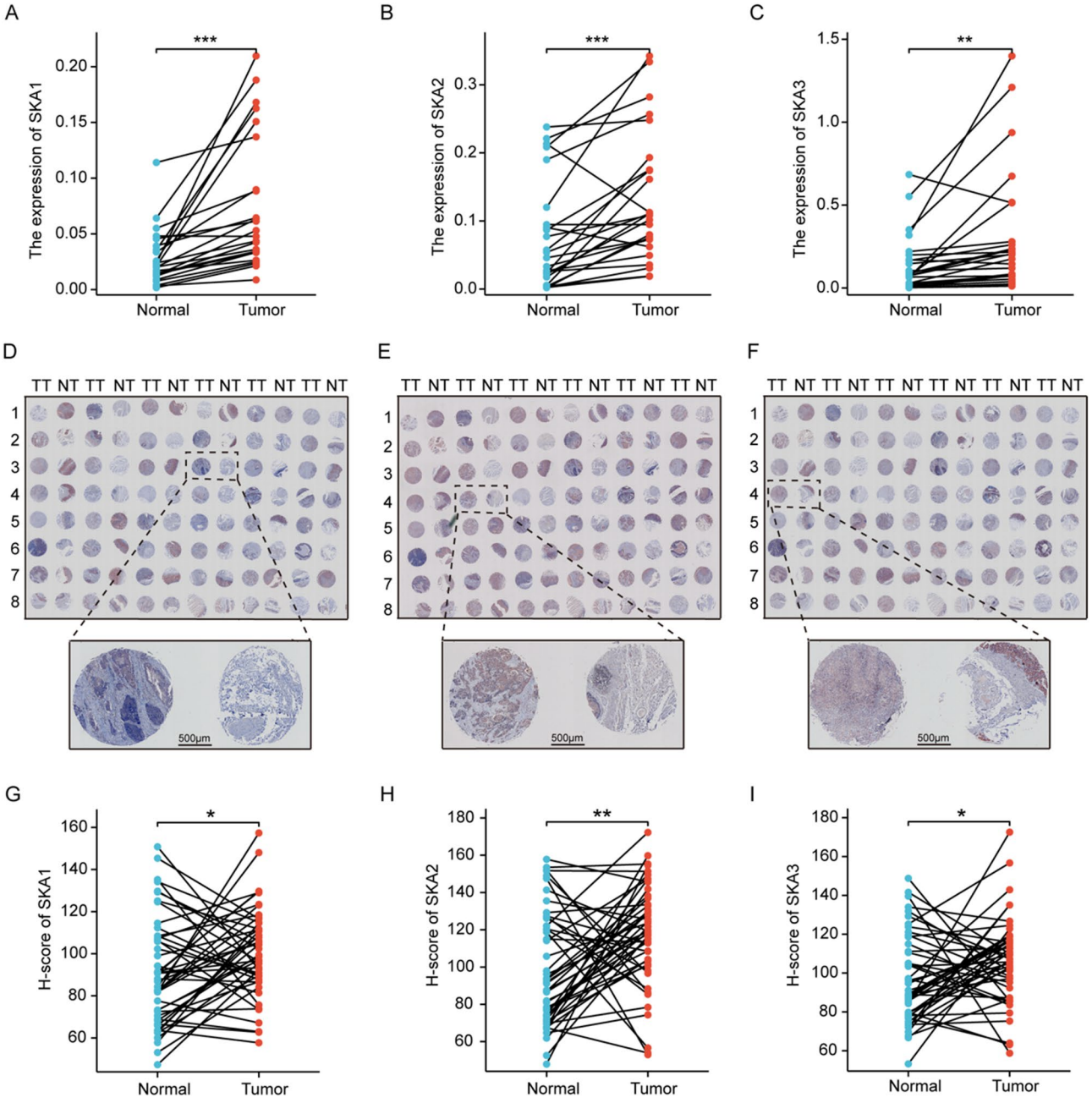


**Fig. 6** Verification of SKA1/2/3 mRNA and protein expression in ESCA specimens (**A-C**) Elevated SKA1/2/3 expression in ESCA tissue samples compared to non-cancerous tissues. (**D-I**) Increased SKA1/2/3 protein expression in ESCA tissue samples compared to non-cancerous tissues by TMA

to the non-cancerous counterparts (Supplementary Fig. 6). Thus, SKA1/12/3 represented elevated expression in ESCA tissues.

#### Knockdown of SKA1/2/3 inhibits cell proliferation with increased apoptosis in ESCA cells

The expression of SKA1/2/3 was significantly reduced in KYSE-150 and KYSE-450 cells upon silencing by siRNA transfection (Fig. 7A-C, Supplementary Fig. 7, Supplementary Fig. 8A-C). Cell proliferation assay by CCK-8 showed that SKA1/2/3 knockdown inhibited cell proliferation in KYSE-150 and KYSE-450 cells (Fig. 7D-F, Supplementary Fig. 8D-F). The flow cytometry analysis revealed obviously increased Annexin $V^+$ cells after SKA1/2/3 silencing in KYSE-150 and KYSE-450 cells (Fig. 7G-H, Supplementary Fig. 8G).

#### Knockdown of SKA1/2/3 impaired cell migration in ESCA cells

The scratch wound healing assays demonstrated that cell migration ability was decreased upon SKA1/2/3 silencing in KYSE-150 and KYSE-450 cells (Fig. 8A-C, Supplementary Fig. 9A-C).

## Discussion

SKA family genes have been discovered to play a role in preserving the integrity of mitosis [15]. Previous reports have documented the different expression of SKA1/2/3 in a variety of malignant tumors, including glioma and HCC [16, 17]. SKA1 was discovered significantly highly expressed in non-small cell lung cancer (NSCLC) with increased cisplatin resistance and lung cancer cell proliferation, invasion and metastasis [18]. Kidney renal clear cell carcinoma (KIRC) cells can proliferate, invade, and migrate when miR-10a-5p selectively regulates the expression of SKA1 [19]. SKA1 can increase the expression of CDC426 and prevent G2/M transition, promoting pancreatic ductal adenocarcinoma (PAAD) growth and migration both in vivo and in vitro [20]. Higher SKA2 expression in breast cancer (BC) is substantially connected with advanced clinical stage and lymph node metastasis, which prevents BC cells from proliferating, invading, and undergoing epithelial-mesenchymal transition (EMT) [21]. SKA2 is strongly expressed in gastric cancer (GC) cells and can be suppressed by miR-520a-3p, preventing GC cells from proliferation and migration [22]. BC patients have elevated SKA3 expression, strongly correlated with poor OS, and BC cell growth is inhibited by SKA3 knockdown via siRNA transfection [23]. Consequently, SKA1/2/3 exhibits distinct expression patterns across various tumor types, potentially influencing the initiation and progression of cancer.

Previous research has reported that SKA3 has been shown to inhibit EMT, which is a key process in tumor progression [24]. Furthermore, the downregulation of SKA3 has been associated with decreased cyclin D1 expression and retinoblastoma phosphorylation, and increased p21 level, suggesting a role in cell cycle regulation and potentially tumor suppression [17]. These findings highlight the multifaceted nature of SKA1/2/3, which can contribute to both cancer progression and tumor suppression depending on the cellular context. SKA1/2/3, as components of the spindle and kinetochore-associated complex, are crucial for stabilizing the centromere-attached spindle microtubules during mid-mitosis, which promotes the completion of mitosis. This function is not only critical in cancer progression but also has implications for tumor suppression, as improper mitotic progression can lead to genomic instability, a hallmark of cancer [25]. Moreover, SKA3 has been shown to be significantly involved in the processes of chromosome cohesion maintenance and silencing of the spindle checkpoint during mitosis, which are essential for preventing abnormal cell division and thus have tumor suppressive properties [4, 26, 27].

Our findings corroborate previous research, indicating that SKA1/2/3 is significantly overexpressed in malignant tumors. The highest expression of SKA1/2 in stage 2 and N1 could be attributed to a variety of factors, including but not limited to, the heterogeneity of the tumor microenvironment, differences in tumor biology at various stages, and potential compensatory mechanisms that come into play as the disease progresses. Thus, greater emphasis will be placed on underscoring the imperative for additional research to gain a comprehensive understanding of these dynamics. Elevated SKA1 expression was linked to poor OS in EAC patients, but with good OS in ESCC patients. Higher expression of SKA2 was associated with unfavorable OS in EAC patients without obvious significance. Increased SKA3 expression was significantly linked to poor OS in patients with EAC as well as OS and RFS in ESCC patients. Additionally, SKA1/2/3 can serve as a potential diagnostic factor with remarkably high accuracy. Therefore, SKA1/2/3 is expected to be a novel biomarker for ESCA, with profound prognostic and diagnostic significance.

The relationship between SKA1/2/3 expression levels and patient prognosis is intricate and subject to a multitude of influences. These include the tumor microenvironment, the genetic diversity within the tumor, and the non-linear impact of these proteins on tumor development. Notably, SKA1/2/3 expression might be influenced by both sex and age, which is an important consideration for understanding the prognosis and treatment outcomes in ESCA patients (Supplementary Fig. 10). ESCC's complexity, stemming from its biological heterogeneity, can result in diverse responses to treatment and the course of the disease. The expression levels of SKA2/3

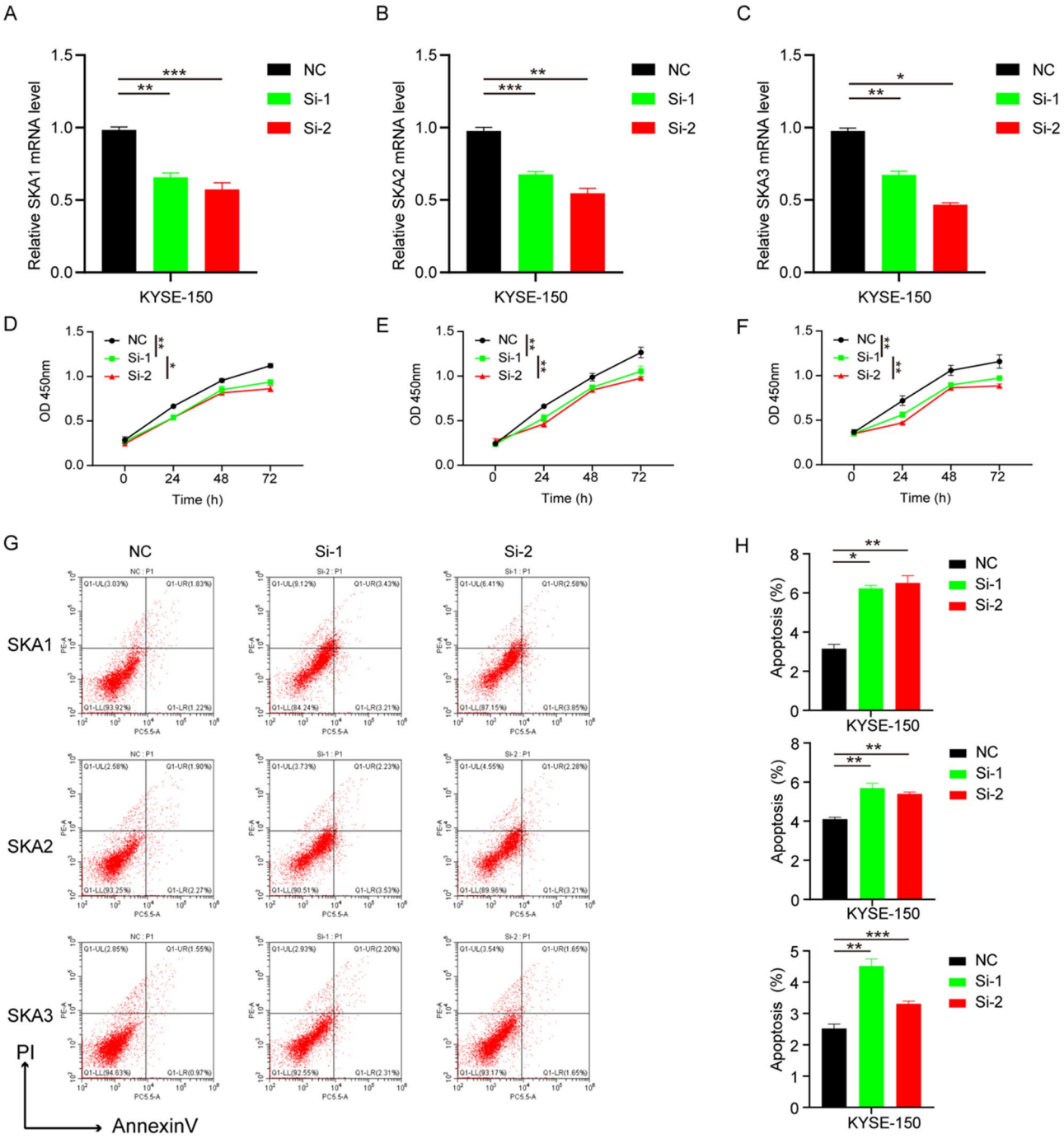


**Fig. 7** Knockdown of SKA1/2/3 inhibits cell proliferation with increased apoptosis in ESCA cells (**A-C**) SKA1/2/3 mRNA expression was significantly reduced in KYSE-150 cells upon silencing by siRNA transfection. Cell proliferation was inhibited in KYSE-150 cells detected by CCK-8 assay (**D-F**). (**G-H**) Flow cytometry analysis showed increased cell apoptosis after Knockdown of SKA1/2/3 by siRNA transfection. $^{**}P < 0.01$; $^{***}P < 0.001$

might modulate particular biological pathways that have a more significant bearing on RFS than on OS. RFS can be affected by treatments administered following the initial recurrence of the disease. It is plausible that patients exhibiting higher levels of SKA2/3 expression could derive greater benefits from these subsequent treatments, potentially enhancing RFS. However, such improvements may not necessarily extend to OS, possibly due to the interference of other underlying factors. Furthermore, the lead-time bias might account for some of the disparities observed. Individuals with elevated SKA2/3 expression might receive an earlier diagnosis, possibly due to more rigorous monitoring or biomarker-guided detection strategies. This could contribute to better RFS outcomes

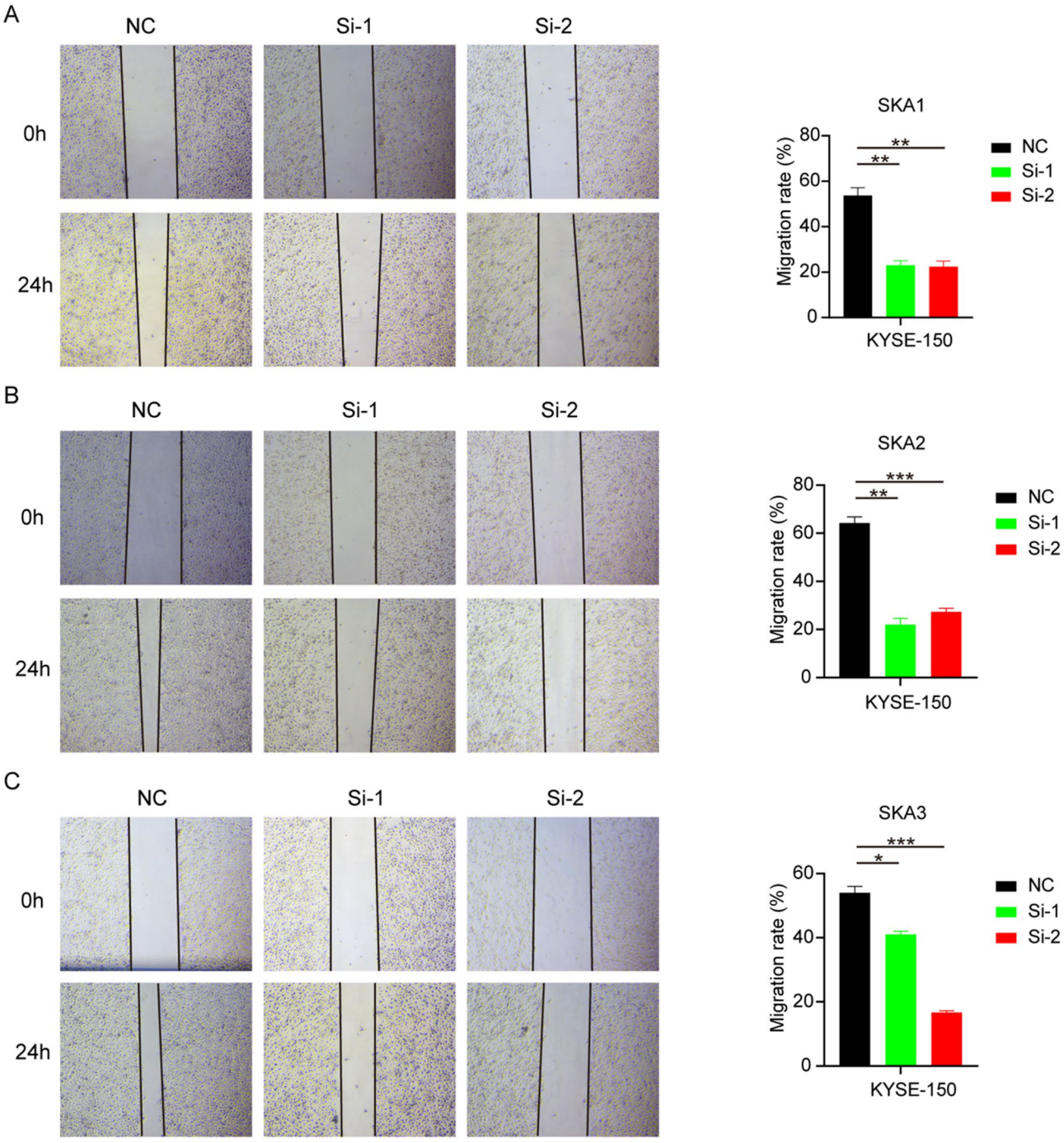


**Fig. 8** Knockdown of SKA1/2/3 impaired cell migration in ESCA cells (**A**)-(**C**) The impaired cell migration of KYSE-150 cells after SKA1/2/3 silencing in scratch wound healing assays. *$P < 0.05$, **$P < 0.01$; ***$P < 0.001$

but may not impact OS. The interaction between SKA2/3 and a range of other biomarkers or genetic elements could also differentially affect RFS and OS. This complex interplay might be responsible for the inconsistencies observed between these two endpoints. Our findings underscore the need for further research to unravel the intricate dynamics at play and to clarify the multifaceted role of SKA2/3 in ESCC prognosis.

The ten hub genes identified and selected in our analysis have been previously reported to be associated with tumorigenesis. HCC has high expression of CDK1, which is strongly associated with patients' OS. In xenograft tumor models of liver cancer, the CDK1 inhibitor RO3306 in combination with sorafenib can considerably slow down tumor progression [28]. Cervical cancer can be inhibited from occurring and developing by targeting

miR-495-3p and miR-143-3p through the concise regulation of CDK1 [29]. The reduction in CCNB2 mRNA levels prevents BC cells from proliferation and migration as well as from entering the G2/M phase of the cell cycle. NSCLC patients have adverse prognoses with CCNB2 overexpression. The miR-335-5p can regulate CCNB2, which in turn affects NSCLC growth, invasion and metastasis [30–32]. CCNA2 is a member of the highly conserved Cyclin family mostly found in the nucleus, with an important cell cycle regulation function linked to DNA replication and cell mitosis [33, 34]. CCNA2 is crucial in cancer development [35]. The elevated expression of CCNA2 in triple-negative breast cancer (TNBC) enhances cell proliferation, invasion and metastasis. Nucleolar and spindle-associated protein1 (NUSAP1) is an important mitotic regulator. And the low expression of CCNA2 may reduce osteosarcoma cell proliferation and cell cycle induction by NUSAP1 [36]. In addition, the cell cycle related 7 genes (CDCA7) can increase the CCNA2 expression, which accelerates the development of ESCC [37]. BUB1B is a specific type of spindle-assembly checkpoint gene crucial for the occurrence and development of BC [38]. Moreover, BUB1B can accelerate the development of extra hepatic cholangio carcinoma (EHCC) by activating the JNK/c-Jun pathway, and mTORC1 signaling pathway in HCC [39]. Previous report has found that BUB1B functions with the zinc finger protein ZNF143 to control glycolysis, which facilitates lung adenocarcinoma (LUAD) cells to grow, spread and invade [40]. In ESCA, the ten selected hub genes exhibited high levels of expression and demonstrated a robust relation with patient prognosis.

Additionally, we have procured tissue samples from 40 ESCA patients and quantified the SKA1/2/3 mRNA levels. Our findings indicate that the expression of SKA1/2/3 is consistently elevated in ESCA tissues compared to the adjacent non-cancerous tissues. We have also conducted an analysis to explore the potential clinical significance of SKA1/2/3 in the etiology and progression of ESCA, as well as its association with carcinogenic signaling pathways. This work aims to offer insights for multi-targeted therapies and interventions that target SKA1/2/3-mediated pathways. However, there remained certain limitations in the present study: (I) The clinical sample size is relatively small, which may affect the generalizability of our findings; (II) A comprehensive understanding of the interactions among SKA family members and their mechanisms in regulating ESCA development and progression is still required; (III) There is an urgent need for further molecular-level validation of the functions of SKA1/2/3. Addressing these limitations will be crucial for future research endeavors, and we are committed to expanding upon these preliminary findings to advance our understanding of ESCA and to develop more effective therapeutic strategies.

In our current study, we have delineated the expression patterns of SKA1/2/3 and their association with the clinicopathological characteristics and prognostic indicators of ESCA. Nevertheless, further in-depth research is warranted to elucidate the exact mechanisms through which SKA1/2/3 contributes to the initiation and progression of ESCA.

## Conclusion

Collectively, our findings highlight a significant overexpression of SKA1/2/3 in ESCA, with higher expression levels strongly correlating with key clinicopathological features and patient outcomes. The enhanced expression of SKA1/2/3 not only suggests its potential as a prognostic biomarker and diagnostic indicator for ESCA but also indicates its promise as a novel therapeutic target. Our study may indeed lay the groundwork for future advancements in early detection and the development of more effective treatment strategies for ESCA.

### Abbreviations

| | |
|---|---|
| ESCA | Esophageal carcinoma |
| SKA1/2/3 | Spindle and kinetochore associated complex subunit |
| KT | Kinetochore |
| PPI | Protein-protein interaction |
| EAC | Esophageal adenocarcinoma |
| ESCC | Esophageal squamous cell carcinoma |
| HCC | Hepatocellular carcinoma |
| LSCC | Laryngeal squamous cell carcinoma |
| PLK1 | Polo-like kinase |
| ROC | Receiver operating characteristic |
| qRT- PCR | Quantitative reverse transcription-polymerase chain reaction |
| CCK-8 | Cell counting kit-8 |
| SD | Standard deviation |
| OS | Overall survival |
| RFS | Recurrence-free survival |
| AUC | Area under the curve |
| TMA | Tissue microarray analysis |
| NSCLC | Non-small cell lung cancer |
| KIRC | Kidney renal clear cell carcinoma |
| PAAD | Pancreatic ductal adenocarcinoma |
| BC | Breast cancer |
| EMT | Epithelial-mesenchymal transition |
| GC | Gastric cancer |
| TNBC | Triple-negative breast cancer |
| NUSAP1 | Nucleolar and spindle-associated protein1 |
| CDCA7 | Cell cycle related 7 genes |
| EHCC | Extra hepatic cholangio carcinoma |
| LUAD | Lung adenocarcinoma |
| GO | Gene ontology |
| KEGG | Kyoto encyclopedia of genes and genomes |

## Supplementary Information

The online version contains supplementary material available at https://doi.org/10.1186/s12885-024-13257-8.

Supplementary Material 1

Supplementary Material 2

Supplementary Material 3

Supplementary Material 4

Supplementary Material 5

Supplementary Material 6

Supplementary Material 7

Supplementary Material 8

Supplementary Material 9

Supplementary Material 10

Supplementary Material 11

Supplementary Material 12

Supplementary Material 13

Supplementary Material 14

**Acknowledgements**
We would like to thank the public database (TCGA, UALCAN, Kaplan-Meier Plotter, STRING and TIMER databases) and everyone involved in this study.

**Author contributions**
CRediT authorship contribution statementLiming Zhang：Writing - original draft, Investigation, Methodology, Formal analysis, Visualization.Shaoqiang Wang: Resources, Software, Data curation, Funding acquisition, Supervision. Lina Wang: Conceptualization, Writing - review & editing, Validation, Funding acquisition, Project administration.

**Funding**
This work was supported by the National Natural Science Foundation of China (81800182, 81802290). The funders had no role in study design, data collection and analysis, decision to publish, or preparation of the manuscript.

**Data availability**
The datasets from TCGA in this study can be found in online databases.

## Declarations

**Ethics approval and consent to participate**
This study was approved by the Ethics Committee of the Affiliated Hospital of Jining Medical University (Approval number 2021-11-C009) in accordance with the Declaration of Helsinki. And written informed consent was obtained before surgery from each patient.

**Consent for publication**
Not applicable.

**Competing interests**
The authors declare no competing interests.

Received: 12 July 2024 / Accepted: 26 November 2024
Published online: 29 November 2024

**References**

1. Arnold M, Soerjomataram I, Ferlay J, Forman D. Global incidence of oesophageal cancer by histological subtype in 2012. Gut. 2015;64(3):381–7.
2. Peng Z, Liu XY, Cheng Z, Kai W, Song Z. Comprehensive analysis of a new immune-related prognostic signature for esophageal cancer and its correlation with infiltrating immune cells and target genes. Ann Transl Med. 2021;9(20):1576.
3. Mao YS, Gao SG, Wang Q, Shi XT, Li Y, Gao WJ, Guan FS, Li XF, Han YT, Liu YY et al. Analysis of a registry database for esophageal cancer from high-volume centers in China. Dis Esophagus 2020, 33(8).
4. Gaitanos TN, Santamaria A, Jeyaprakash AA, Wang B, Conti E, Nigg EA. Stable kinetochore-microtubule interactions depend on the Ska complex and its new component Ska3/C13Orf3. Embo j. 2009;28(10):1442–52.
5. Hanisch A, Silljé HH, Nigg EA. Timely anaphase onset requires a novel spindle and kinetochore complex comprising Ska1 and Ska2. Embo j. 2006;25(23):5504–15.
6. Tian F, Xing X, Xu F, Cheng W, Zhang Z, Gao J, Ge J, Xie H. Downregulation of SKA1 gene expression inhibits cell growth in human bladder Cancer. Cancer Biother Radiopharm. 2015;30(7):271–7.
7. Dong C, Wang XL, Ma BL. Expression of Spindle and Kinetochore-Associated Protein 1 Is Associated with Poor Prognosis in Papillary Thyroid Carcinoma. *Dis Markers* 2015, 2015:616541.
8. Wang D, Suo YJ, Gong L, Lv SQ. SKA2 promotes proliferation and invasion of hepatocellular carcinoma cells via activating the β-catenin signaling pathway. Neoplasma. 2020;67(4):743–50.
9. Gao W, Zhang Y, Luo H, Niu M, Zheng X, Hu W, Cui J, Xue X, Bo Y, Dai F, et al. Targeting SKA3 suppresses the proliferation and chemoresistance of laryngeal squamous cell carcinoma via impairing PLK1-AKT axis-mediated glycolysis. Cell Death Dis. 2020;11(10):919.
10. Chandrashekar DS, Bashel B, Balasubramanya SAH, Creighton CJ, Ponce-Rodriguez I, Chakravarthi B, Varambally S. UALCAN: a portal for facilitating Tumor Subgroup Gene expression and survival analyses. Neoplasia. 2017;19(8):649–58.
11. Nagy Á, Munkácsy G, Győrffy B. Pancancer survival analysis of cancer hallmark genes. Sci Rep. 2021;11(1):6047.
12. von Mering C, Huynen M, Jaeggi D, Schmidt S, Bork P, Snel B. STRING: a database of predicted functional associations between proteins. Nucleic Acids Res. 2003;31(1):258–61.
13. Lopes CT, Franz M, Kazi F, Donaldson SL, Morris Q, Bader GD. Cytoscape web: an interactive web-based network browser. Bioinformatics. 2010;26(18):2347–8.
14. Li T, Fan J, Wang B, Traugh N, Chen Q, Liu JS, Li B, Liu XS. TIMER: a web server for Comprehensive Analysis of Tumor-infiltrating Immune cells. Cancer Res. 2017;77(21):e108–10.
15. Sivakumar S, Janczyk P, Qu Q, Brautigam CA, Stukenberg PT, Yu H, Gorbsky GJ. The human SKA complex drives the metaphase-anaphase cell cycle transition by recruiting protein phosphatase 1 to kinetochores. Elife. 2016;5:e12902.
16. Wang X, Zeng Y, Zhou M, Zhang X, Xu A, Lin J, Wu Z, Xie C, Luo J, Ding S, et al. SKA1 promotes malignant phenotype and progression of glioma via multiple signaling pathways. Cancer Cell Int. 2019;19:324.
17. Hou Y, Wang Z, Huang S, Sun C, Zhao J, Shi J, Li Z, Wang Z, He X, Tam NL, et al. SKA3 promotes tumor growth by regulating CDK2/P53 phosphorylation in hepatocellular carcinoma. Cell Death Dis. 2019;10(12):929.
18. Shen L, Yang M, Lin Q, Zhang Z, Miao C, Zhu B. SKA1 regulates the metastasis and cisplatin resistance of non-small cell lung cancer. Oncol Rep. 2016;35(5):2561–8.
19. Arai T, Okato A, Kojima S, Idichi T, Koshizuka K, Kurozumi A, Kato M, Yamazaki K, Ishida Y, Naya Y, et al. Regulation of spindle and kinetochore-associated protein 1 by antitumor miR-10a-5p in renal cell carcinoma. Cancer Sci. 2017;108(10):2088–101.
20. Li T, Liu X, Xu B, Wu W, Zang Y, Li J, Wei L, Qian Y, Xu H, Xie M, et al. SKA1 regulates actin cytoskeleton remodelling via activating Cdc42 and influences the migration of pancreatic ductal adenocarcinoma cells. Cell Prolif. 2020;53(4):e12799.
21. Wang Y, Zhang C, Mai L, Niu Y, Wang Y, Bu Y. PRR11 and SKA2 gene pair is overexpressed and regulated by p53 in breast cancer. BMB Rep. 2019;52(2):157–62.
22. Su H, Ren F, Jiang H, Chen Y, Fan X. Upregulation of microRNA-520a-3p inhibits the proliferation, migration and invasion via spindle and kinetochore associated 2 in gastric cancer. Oncol Lett. 2019;18(3):3323–30.
23. Tang D, Zhao X, Zhang L, Wang Z, Wang C. Identification of hub genes to regulate breast cancer metastasis to brain by bioinformatics analyses. J Cell Biochem. 2019;120(6):9522–31.
24. Zhang C, Zhao S, Tan Y, Pan S, An W, Chen Q, Wang X, Xu H. The SKA3-DUSP2 Axis promotes gastric Cancer Tumorigenesis and epithelial-mesenchymal transition by activating the MAPK/ERK Pathway. Front Pharmacol. 2022;13:777612.
25. Chen C, Guo Q, Song Y, Xu G, Liu L. SKA1/2/3 serves as a biomarker for poor prognosis in human lung adenocarcinoma. Transl Lung Cancer Res. 2020;9(2):218–31.
26. Daum JR, Wren JD, Daniel JJ, Sivakumar S, McAvoy JN, Potapova TA, Gorbsky GJ. Ska3 is required for spindle checkpoint silencing and the maintenance of chromosome cohesion in mitosis. Curr Biol. 2009;19(17):1467–72.

27. Theis M, Slabicki M, Junqueira M, Paszkowski-Rogacz M, Sontheimer J, Kittler R, Heninger AK, Glatter T, Kruusmaa K, Poser I, et al. Comparative profiling identifies C13orf3 as a component of the Ska complex required for mammalian cell division. Embo j. 2009;28(10):1453–65.
28. Wu CX, Wang XQ, Chok SH, Man K, Tsang SHY, Chan ACY, Ma KW, Xia W, Cheung TT. Blocking CDK1/PDK1/β-Catenin signaling by CDK1 inhibitor RO3306 increased the efficacy of sorafenib treatment by targeting cancer stem cells in a preclinical model of hepatocellular carcinoma. Theranostics. 2018;8(14):3737–50.
29. Tang J, Pan H, Wang W, Qi C, Gu C, Shang A, Zhu J. MiR-495-3p and mir-143-3p co-target CDK1 to inhibit the development of cervical cancer. Clin Transl Oncol. 2021;23(11):2323–34.
30. Tang Q, Li W, Zheng X, Ren L, Liu J, Li S, Wang J, Du G. MELK is an oncogenic kinase essential for metastasis, mitotic progression, and programmed death in lung carcinoma. Signal Transduct Target Ther. 2020;5(1):279.
31. Wang X, Xiao H, Wu D, Zhang D, Zhang Z. Mir-335-5p regulates cell cycle and metastasis in Lung Adenocarcinoma by Targeting CCNB2. Onco Targets Ther. 2020;13:6255–63.
32. Qian X, Song X, He Y, Yang Z, Sun T, Wang J, Zhu G, Xing W, You C. CCNB2 overexpression is a poor prognostic biomarker in Chinese NSCLC patients. Biomed Pharmacother. 2015;74:222–7.
33. Silva Cascales H, Burdova K, Middleton A, Kuzin V, Müllers E, Stoy H, Baranello L, Macurek L, Lindqvist A. Cyclin A2 localises in the cytoplasm at the S/G2 transition to activate PLK1. Life Sci Alliance 2021, 4(3).
34. Zhang QH, Yuen WS, Adhikari D, Flegg JA, FitzHarris G, Conti M, Sicinski P, Nabti I, Marangos P, Carroll J. Cyclin A2 modulates kinetochore-microtubule attachment in meiosis II. J Cell Biol. 2017;216(10):3133–43.
35. Yang F, Hu Y, Liu HX, Wan YJ. MiR-22-silenced cyclin A expression in colon and liver cancer cells is regulated by bile acid receptor. J Biol Chem. 2015;290(10):6507–15.
36. Li T, Liu D, Li C, Ru L, Wang X. Silencing of LncRNA AFAP1-AS1 inhibits cell proliferation in oral squamous Cancer by suppressing CCNA2. Cancer Manag Res. 2021;13:7897–908.
37. Li H, Weng Y, Wang S, Wang F, Wang Y, Kong P, Zhang L, Cheng C, Cui H, Xu E, et al. CDCA7 facilitates Tumor Progression by directly regulating CCNA2 expression in esophageal squamous cell carcinoma. Front Oncol. 2021;11:734655.
38. Deng H, Cheng Y, Guo Z, Zhang F, Lu X, Feng L, Wang X, Xu Z. Overexpression of CyclinA2 ameliorates hypoxia-impaired proliferation of cardiomyocytes. Exp Ther Med. 2014;8(5):1513–7.
39. Zhong C, Han Y, Ma J, Zhang X, Sun M, Wang Y, Chen J, Mi W, Xu X, Qiu J. Viral-mediated expression of c-Myc and cyclin A2 induces cochlear progenitor cell proliferation. Neurosci Lett. 2015;591:93–8.
40. Zhou X, Yuan Y, Kuang H, Tang B, Zhang H, Zhang M. BUB1B (BUB1 mitotic checkpoint Serine/Threonine kinase B) promotes lung adenocarcinoma by interacting with zinc finger protein ZNF143 and regulating glycolysis. Bioengineered. 2022;13(2):2471–85.

## Publisher's note